JOURNAL OF THERMOPHYSICS AND HEAT TRANSFER
Vol. 16, No. 4, October–December 2002

Optimization of Micro Heat Pipe Radiators in a Radiation Environment

Y. X. Wang* and G. P. Peterson†
Rensselaer Polytechnic Institute, Troy, New York 12180

A combined numerical and experimental investigation was conducted to predict, measure, and optimize the heat transfer performance of a novel micro heat pipe radiator design that utilized an array of metal wires sandwiched between two thin sheets. The numerical model indicated that the maximum heat transport capacity for a single micro heat pipe increases proportionally to the square of the wire diameter, that the optimal charge volume decreased with increasing heat flux, that the maximum heat transport capacity increases with increases in the wire spacing, and that the overall maximum heat transport capacity of the radiator is strongly governed by the spacing of the wires, the length of the radiator, and the radiation capacity of the radiator surface. These numerical results are consistent with the experimental results, which indicated that the uniformity of the temperature distribution and the radiation efficiency both increased with increasing wire diameter, resulting in a maximum heat transport capacity for radiators utilizing a wire diameter of 0.635 mm of 15.2 W. Additional experimental tests conducted on radiators utilizing wire diameters of 0.813 and 1.016 mm illustrated similar trends; however, for micro heat pipes with wire diameters larger than 0.813 mm, the maximum heat transport capacity was not reached within the operating temperature of the acetone working fluid. Comparison of the proposed micro heat pipe radiators with solid conductors and uncharged versions indicated significant improvements in the temperature uniformity and overall radiation efficiency. A maximum radiation efficiency of 0.95 was observed.

Nomenclature

A	=	surface area of the radiator, m^2
$A_{c,l}$	=	liquid-phase cross-sectional area, m^2
$A_{c,v}$	=	vapor-phase cross-sectional area, m^2
A_r	=	surface area of the radiator, m^2
d_w	=	wire diameter, m
F	=	view factor
g	=	gravitational acceleration, m/s^2
$h_{c,o}$	=	heat transfer coefficient outside of the condenser, J/m^2 K
h_{fg}	=	latent heat of vaporization, J/kg
$\bar{h}_c$	=	average heat transfer coefficient in the condenser, J/m^2 K
L	=	length of the micro heat pipe, m
m_l	=	liquid mass flow rate, kg/s
m_v	=	vapor mass flow rate, kg/s
P_c	=	capillary pressure, Pa
P_l	=	liquid-phase pressure, Pa
P_{sat}	=	saturated pressure, Pa
P_v	=	vapor-phase pressure, Pa
p	=	perimeter, m
$Q_{\max}$	=	maximum heat transport capacity, W
$Q_{\max,r}$	=	maximum radiation transport capacity, W
q''	=	heat flux per unit area, W/m^2
Re	=	Reynolds number
R_w	=	radius of the wire, m
r_m	=	radius of the liquid meniscus, m
T	=	temperature, K
T_{sink}	=	sink temperature, K
T_v	=	vapor temperature, K
$T_{w,o}$	=	outside temperature of the wall, K
u_l	=	liquid velocity in the x-direction, m/s
u_v	=	vapor velocity in the x-direction, m/s
$v_{l,i}$	=	liquid velocity at the interface, m/s
$v_{v,i}$	=	vapor velocity at the interface, m/s
w	=	width of a single heat pipe, m
α	=	contact angle, deg
ε	=	emissivity
η_{rad}	=	radiation efficiency, %
θ	=	inclination angle, deg
ρ_l	=	liquid density, kg/m^3
ρ_v	=	vapor density, kg/m^3
σ	=	surface tension, N/m
σ_0	=	radiation constant, 5.67×10^{-8} W/(m$^2 \cdot$ K^4)
τ	=	shear stress, N/m^2

Subscripts

c	=	condenser
e	=	evaporator
i	=	interface
l	=	liquid phase
m	=	meniscus
max	=	maximum
sink	=	heat sink
v	=	vapor phase

Received 7 February 2002; revision received 11 April 2002; accepted for publication 28 May 2002.

*Research Assistant Professor, Department of Mechanical, Aeronautical, and Nuclear Engineering, Office of the Provost, Room 3018, Troy Building. Member AIAA.

†Professor of Mechanical Engineering, Department of Mechanical, Aeronautical, and Nuclear Engineering, Fellow AIAA.

Introduction

IN an effort to develop a flexible, lightweight radiator for long-term manned missions, a wire-bonded micro heat pipe radiator was proposed to improve the radiation efficiency and, therefore, reduce the weight of the spacecraft.[1] This micro heat pipe radiator was fabricated by bonding an array of parallel aluminum wires between two thin aluminum sheets or laminates. The sharp corners formed at the intersection of the wires and the sheets serve as liquid arteries and "pump" the working fluid from the condenser to the evaporator. The vapor flows in the channels formed between the individual wires as illustrated in Fig. 1. In addition to providing capillary pumping, the presence of the wires also assists in freeze

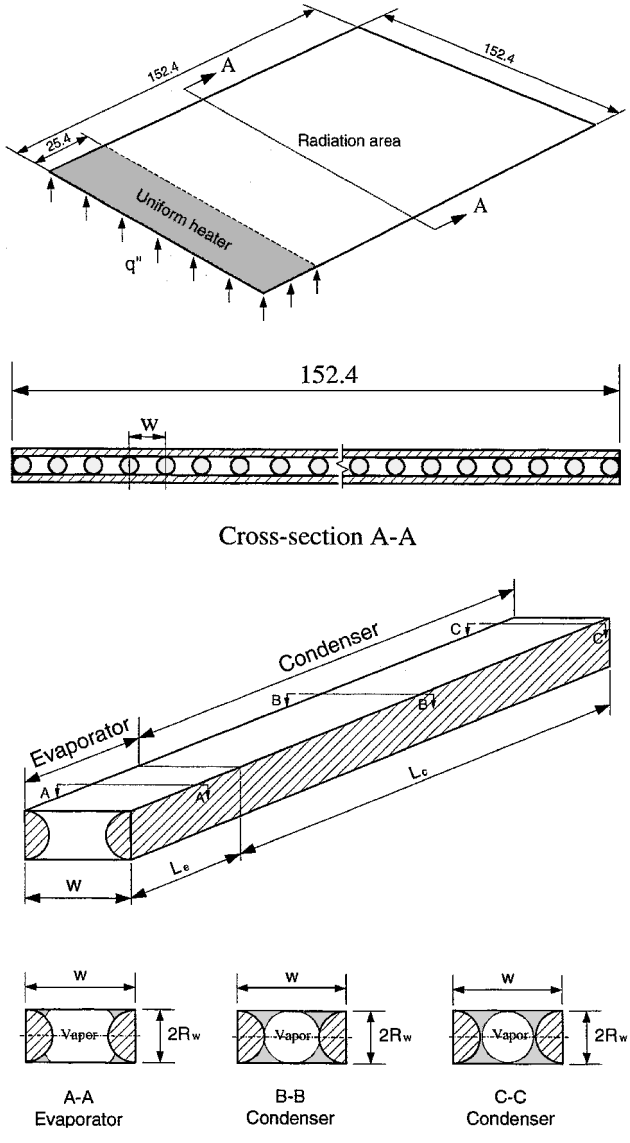

Fig. 1 Micro heat pipe radiator fabrication.

prevention and recovery. Acetone was used as the working fluid in the current research work, although ammonia may be more suitable for higher-power spacecraft applications.

To predict the heat transfer performance and operational limitations, as well as optimize the micro heat pipe radiator in radiation environments, a detailed analytical model was developed. Once the model was completed, an experimental test facility was developed and an experimental investigation conducted to verify the veracity of this new concept and the numerical model. In most of the relevant studies, theoretical and/or experimental investigations have been conducted to better understand the effect of continued size reductions of micro heat pipes, determine the effective thermal conductivity, and examine the transient operational characteristics and performance limitations. These studies included a combined steady-state analytical and experimental investigation of a heat pipe approximately 1 mm^2 in cross-sectional area,[2] a transient numerical investigation of a similar device,[3] a transient investigation of micro-heat-pipes specifically designed for the cooling of ceramic chip carriers,[4] and the evaluation of individual micro heat pipes etched or otherwise fabricated into silicon wafers.[5] Ma and Peterson[6] experimentally studied the maximum unit effective area heat transport capacity in triangular grooves based on the capillary limit. The experimental results indicated that increasing the tilt angle and wetted length resulted in a significant decrease in heat transport and unit effective area heat transport. Longtin et al.[7] studied micro heat pipes with triangular grooves using a one-dimensional model to predict the transport limitation. However, the analysis did not consider the fluid flow in the condenser section, rendering it of little use in applications such as the current one, where the condenser section is very long compared to the combined length of the evaporator and adiabatic sections. In addition, determination of the initial radius of the liquid meniscus at the evaporator cannot be determined directly.

Although there have been many investigations of micro heat pipes in convection environments, there is little information as to how these devices will function in a radiation environment. In the current application, the performance of the radiator will be strongly affected by the sink temperature and radiator surface characteristics. Furthermore, because the condenser section is exposed to a radiation environment, the heat flux and the temperature may not be uniform. Based on the physical characteristics of the micro heat pipe, a detailed one-dimensional analytical model, which takes into consideration the variation of the cross-sectional area of the liquid and vapor phase and the influence of the vapor phase on the liquid friction factor has been established to predict the maximum heat transport capacity, optimum charging volume, and effective thermal conductivity of the micro heat pipes in a radiation environment.

Experimental Test Program

The operation of a micro heat pipe in a radiation environment is different from that occurring in a convection environment[1] in that 1) the operating temperature of the micro heat pipe depends on the sink temperature and 2) the heat flux in the condenser section is not uniform and depends on the temperature of the radiator surface. As a result, the maximum heat transport capacity and operational behavior may be different from that occurring in a convective environment. To determine the maximum heat transport capacity, a series of experimental test articles, shown in Fig. 1, was developed. Heat was added to the evaporator section uniformly using an electrical resistance heater and dissipated to the environment from the condenser section by radiation. Power input to the evaporator and the temperature distributions on the outer surface of the micro heat pipe were measured to determine the maximum heat transport capacity and radiation efficiency. To determine the effect of the geometric parameters of the channels on the maximum capillary transport capacity, micro heat pipe radiators with different wire diameters and channel widths were fabricated and tested.

The micro heat pipe radiators were fabricated by brazing a parallel array of aluminum wires between two thin aluminum sheets. The sharp corner regions formed between the wires and the sheets serve as liquid arteries to pump the working fluid, acetone, from the condenser section to the evaporator section. The vapor flows in the channels formed between the individual wires. In addition to providing capillary pumping, the solid wires were also helpful in assisting in freeze prevention and recovery. Several micro heat pipe radiators with different wire diameters were fabricated. The details of these various test articles are listed in Table 1.

The experimental test facility, shown in Fig. 2, was developed to conduct a series of experiments designed to determine the maximum heat transport capacity and temperature distribution of the micro heat pipe radiators under various test conditions. This system consisted of a vacuum chamber, a vacuum system, a cooling system, two copper cold plates, a power supply and a measuring unit, a data acquisition system, and a computer. The experiments were conducted in a closed, round stainless steel vacuum chamber with dimensions of 720×240 mm. The chamber was evacuated with a mechanical vacuum pump that was used to maintain a vacuum of 10^{-3} torr to reduce the convection heat loss to the test environment. The cooling system consisted of a cooling bath and a liquid nitrogen Dewar. Cooling fluid flowing through the cold plates provided the low-temperature radiative environment. With this system, the temperature on the surface of the cold plate could reach a temperature as low as 200 K, and a uniform temperature distribution could be maintained to within ± 1.0°C. The cold plates were made of square copper sheets 457.2×457.2 mm and 0.5 mm thick onto which a series of parallel copper cooling tubes had been silver soldered. The plates were painted with a "black" paint to improve the absorptivity of the surface. A high-quality insulation and one layer of highly

Table 1 Configurations for the tested micro heat pipe radiators

Prototype	TA1[a]	TA2[a]	TA3[a]	TA4[a]
Material	Aluminum	Aluminum	Aluminum	Aluminum
Working fluid	Acetone	Acetone	Acetone	No
Total dimension, mm	152.4 × 152.4	152.4 × 152.4	152.4 × 152.4	152.4 × 152.4
Thickness of sheet, mm	0.406	0.406	0.406	0.406
Diameter of wire, mm	0.635	0.813	1.016	0.635
Number of wires	77	84	73	77
W, mm	2.0	1.8	2.1	2.0
Evaporator size, mm	25.4	25.4	25.4	25.4
Condenser size, mm	127.0	127.0	127.0	127.0
Charging volume, ml	2.0	2.9	4.3	No
Thermocouples	27	27	27	27

[a]As presented in Ref. 12.

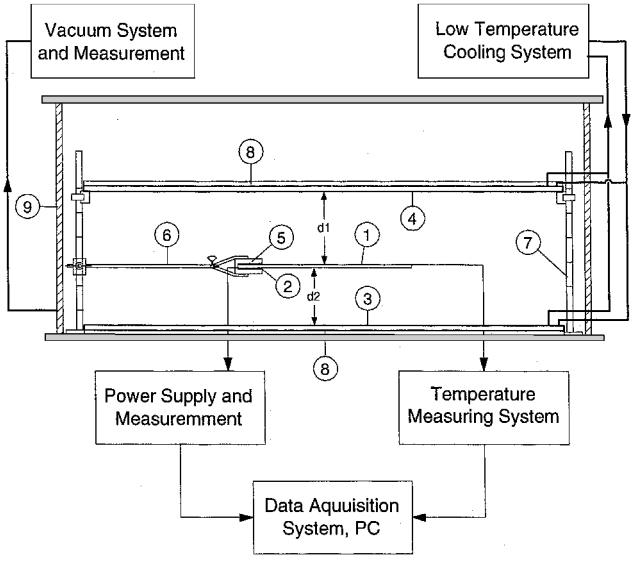

1. Micro heat pipe radiator 2. Electric heater
3. Bottom cold plate 4. Top cold plate
5. Electric heater insulation 6. Support level
7. Adjustable support feet 8. Insulation material
9. Vacuum chamber

Fig. 2 Schematic of the test facility.

reflective material were applied to the top of the plates to prevent parasitic heat losses and obtain a more uniform temperature distribution. The test article was then placed horizontally between the two cold plates.

Four thin film electric heaters (76.2 × 25.4 mm) were attached to both sides of the evaporator section of the heat pipe, as shown in Fig. 1, and the power added to the heaters was measured and recorded by the data acquisition system. The radiator was held in position by insulating clamps designed to allow the distance between the radiator and cold plates to be adjusted and controlled. Insulation material was placed between the clamp and the radiator to prevent heat loss by conduction. Attached to the outer surface of the micro heat pipe radiator to measure the temperature distribution, using highly conductive silver epoxy, were 27 T-type thermocouples (AWG-40). In addition, another 10 thermocouples were attached to the surfaces of the cold plates to monitor the temperatures and 5 thermocouples were located on the walls of the vacuum chamber.

Experimental Procedure

Before each set of tests, the vacuum chamber was evacuated and maintained at a constant vacuum environment. Throughout the entire test program, the vacuum pressure was maintained at less than 10^{-3} torr, and the temperature of the cooling system was maintained at a constant value.

In the test procedure, the heat pipe radiator was placed between the two cold plates, and the space between the radiator and the cold plates, along with the orientation of the heat pipe, was checked and verified. The chamber was then evacuated and the coolant turned on. Once the system had reached equilibrium (i.e., the chamber had been evacuated and the temperature on the two cold plates was uniform), the power supply was activated and the power input was increased slightly. Throughout the tests, the temperatures on the radiator surface were observed and recorded. When the system reached steady state, defined as the point where the temperatures on the radiator surface did not vary more than 0.5 deg in 10 min (approximately 30–50 min), the input power and temperatures on the micro heat pipe radiator, cold plates, and vacuum chamber were recorded and the power incremented. The power input was continuously increased until the temperature at the end of the evaporator section increased sharply and dryout occurred. The coolant temperature was then reset, and the preceding steps were repeated to obtain another set of data.

Throughout the test program, the operating temperature of the micro heat pipe radiator was maintained at a value of less than 80°C to protect the heat pipe from overpressurizing. Because the tests were conducted in a vacuum environment, the pressure difference between the inside and outside of the heat pipe was 1 bar higher than that obtained for the convection environment.

Data Reduction

It is helpful at this point to introduce the concept of radiation efficiency to determine the effectiveness of the radiators. The radiation efficiency is defined here as the actual radiation heat transport rate divided by the maximum possible heat radiation transport rate at the same evaporating (source) temperature. The maximum possible radiation transport rate of a radiator is reached when the radiator has a uniform temperature, that is, the radiator has an infinite thermal conductivity. This means that the more uniform the temperature distribution, the higher the radiation efficiency. This definition can be expressed as

$$\eta_{\text{rad}} = Q_{\text{act}}/Q_{\max,r} \tag{1}$$

where

$$Q_{\text{act}} = \sigma_0 \int_A F\varepsilon\left(T^4 - T_{\sin k}^4\right) \mathrm{d}A \tag{2}$$

$$Q_{\max,r} = \sigma_0 \int_A F\varepsilon\left(T_{\max}^4 - T_{\sin k}^4\right) \mathrm{d}A \tag{3}$$

Substituting Eqs. (2) and (3) into Eq. (1) yields

$$\eta_{\text{rad}} = \frac{Q_{\text{act}}}{Q_{\max,r}} = \frac{1}{A\left(T_{\max}^4 - T_{\sin k}^4\right)} \int_A \left(T^4 - T_{\sin k}^4\right) \mathrm{d}A \tag{4}$$

If the temperature across the radiator is uniform, the radiation efficiency becomes

$$\eta_{\text{rad}} = \frac{1}{L}\int_0^L \frac{\left(T^4 - T_{\text{sin}\,k}^4\right)}{\left(T_{\max}^4 - T_{\text{sin}\,k}^4\right)}\,\mathrm{d}x \tag{5}$$

For solid radiators, that is, metal or carbon fiber radiators, the higher the thermal conductivity, the more uniform the temperature and, therefore, the higher the radiation efficiency. When the temperature on the radiator is completely uniform, the radiation efficiency of the radiator is unity.

Analytical Model

As presented previously by Wang and Peterson,[8] an analytical model was developed to predict the heat transfer performance and optimize the physical parameters of the micro heat pipe radiator. With this model, the capillary limitation was found to be the dominant limitation for moderate or low-temperature heat pipes,[1,8–12] and, hence, the two-phase flow and heat transfer occurring in the micro channels of the heat pipe radiator are governed by mass, momentum, and energy conservation:

$$\frac{\mathrm{d}\dot{m}_l}{\mathrm{d}x} - \rho_l v_{i,l} p_{i,l} = 0 \tag{6}$$

$$\frac{\mathrm{d}\dot{m}_v}{\mathrm{d}x} - \rho_v v_{i,v} p_{i,v} = 0 \tag{7}$$

$$-\left[\dot{m}_l\frac{\mathrm{d}u_l}{\mathrm{d}x} + u_l\frac{\mathrm{d}\dot{m}_l}{\mathrm{d}x}\right] - A_{c,l}\frac{\mathrm{d}P_l}{\mathrm{d}x} + p_l\tau_l - g\rho_l A_{c,l}\sin\theta = 0 \tag{8}$$

$$\dot{m}_v\frac{\mathrm{d}u_v}{\mathrm{d}x} + u_v\frac{\mathrm{d}\dot{m}_v}{\mathrm{d}x} + A_{c,v}\frac{\mathrm{d}P_v}{\mathrm{d}x} + p_v\tau_v + g\rho_v A_{c,v}\sin\theta = 0 \tag{9}$$

where $\dot{m}_l = \rho_l u_l A_{c,l}$ and $\dot{m}_v = \rho_v u_v A_{c,v}$. In this expression, both the liquid and vapor flows are assumed to be fully developed. The capillary pressure produced at the liquid–vapor interface in the micro channels can be calculated by the Laplace–Young differential equation,

$$\frac{\mathrm{d}P_v}{\mathrm{d}x} - \frac{\mathrm{d}P_l}{\mathrm{d}x} = -\frac{\sigma}{r_m^2}\frac{\mathrm{d}r}{\mathrm{d}x} \tag{10}$$

For the present situation, in which the condenser section is exposed to a radiation environment as opposed to a convective environment, the energy conservation equation of the liquid phase can be simplified as

$$v_{i,l} = \begin{cases} \dfrac{2q_e'' w}{\rho_l p_{i,l} h_{fg}} & \text{evaporator section} \\ \dfrac{2wh_{c,o}(T_v - T_{\text{sin}\,k})(1 + h_{c,o}/\bar{h}_c)^{-1}}{\rho_l p_{l,i} h_{fg}} & \text{condenser section} \end{cases} \tag{11}$$

where q_e'' is assumed to be the uniform heat flux added to the evaporator section and $h_{c,o}$ is the radiation heat transfer coefficient on the outer surface, which can be expressed as

$$h_{c,o} = \varepsilon\sigma_0(T_{w,o} + T_{\text{sin}\,k})\left(T_{w,o}^2 + T_{\text{sin}\,k}^2\right) \tag{12}$$

Similarly, the energy conservation equation for the vapor phase is given as follows:

$$v_{i,v} = \begin{cases} \dfrac{2q_e'' w}{\rho_v p_{i,v} h_{fg}} & \text{evaporator section} \\ \dfrac{2wh_{c,o}(T_v - T_{\text{sin}\,k})(1 + h_{c,o}/\bar{h}_c)^{-1}}{\rho_v p_{i,v} h_{fg}} & \text{condenser section} \end{cases} \tag{13}$$

Because the heat transfer resistance of the outer surface of the radiator is much larger than the heat transfer resistance through the interface, that is, $h_{c,o}/\bar{h}_c \ll 1$, as shown in Table 2, this term can be neglected.

Table 2 Comparison of heat transfer coefficients

Case	T_{sink}, K	T_v, K	$h_{c,o}$, W/m^{2}K	$\bar{h}_c$ (Ref. 1), W/m^{2}K	$h_{c,o}/\bar{h}_c$
1	273	293	5.15	≥5000	≤0.0010
2	273	313	5.73	≥5000	≤0.0011
3	273	353	7.07	≥5000	≤0.0014
4	0	293	1.43	≥5000	≤0.0003
5	0	313	1.74	≥5000	≤0.0004
6	0	353	2.49	≥5000	≤0.0005

The geometric parameters in Eqs. (6–13) can be obtained by assuming a constant liquid meniscus radius in the microchannel as presented in Ref. 8. As was the case for the convective environment, the liquid- and vapor-phase frictional factors in a radiation environment are similar to those presented by Wang and Peterson.[8]

Numerical Treatment

The boundary conditions required to solve the five first-order, nonlinear, coupled ordinary differential equations along with the treatment of these boundary conditions are similar to those presented in Ref. 8. At the end of the condenser section ($x = L_t$), the boundary conditions can be expressed as

$$u_l = u_v = 0 \tag{14}$$

$$r_m = r_{m,\max} \tag{15}$$

$$P_v = P_{\text{sat}}(T_v) \tag{16}$$

$$P_l = P_v - \sigma/r_{m,\max} \tag{17}$$

If there is no extra working fluid present in the condenser, the maximum meniscus radius occurs in the microchannels at the end of the condenser, where the film condensate meets at the midpoint of the wire. The radius for this particular configuration can be estimated as

$$r_{m,\max} = R_w/(\cos\alpha - \sin\alpha) \tag{18}$$

A fourth-order Runge–Kutta method was used to solve the five first-order differential equations with the boundary conditions described in Eqs. (14–17). The environment for this particular application is such that the condenser is exposed to a pure radiation environment, where neither the heat flux nor the temperature is constant. The heat flux depends on the outer surface temperature of the heat pipe, and the initial temperature or pressure at the end of the condenser is not known. Therefore, an initial temperature must be assumed, and the corresponding pressure, velocity, liquid profile, and heat transfer coefficient calculated. The total radiation power must then be compared to the power input in the evaporation section. A FORTRAN program was written to calculate all of the parameters needed by using the Runge–Kutta method and the bisection method. The main procedures are listed hereafter:

1) Estimate the initial temperature of vapor at the end of condenser.

2) Find the initial pressure of the vapor by correlation of the temperature and pressure of the saturated vapor, maximum meniscus radius of the liquid surface, and liquid pressure using Eqs. (14–17).

3) Calculate the liquid pressure, vapor pressure, liquid velocity, vapor velocity, and liquid meniscus radius using Eqs. (6–10) for a given step size.

4) Calculate the radiation heat transfer coefficient and outside temperature using Eq. (12).

5) Integrate the radiation heat transfer along the condenser section and compare the total radiation heat out and heat input from the evaporator.

6) Use the bisection method and iterate until the difference of the radiation heat transfer and the power input is small enough to achieve the desired accuracy to obtain an accurate temperature distribution.

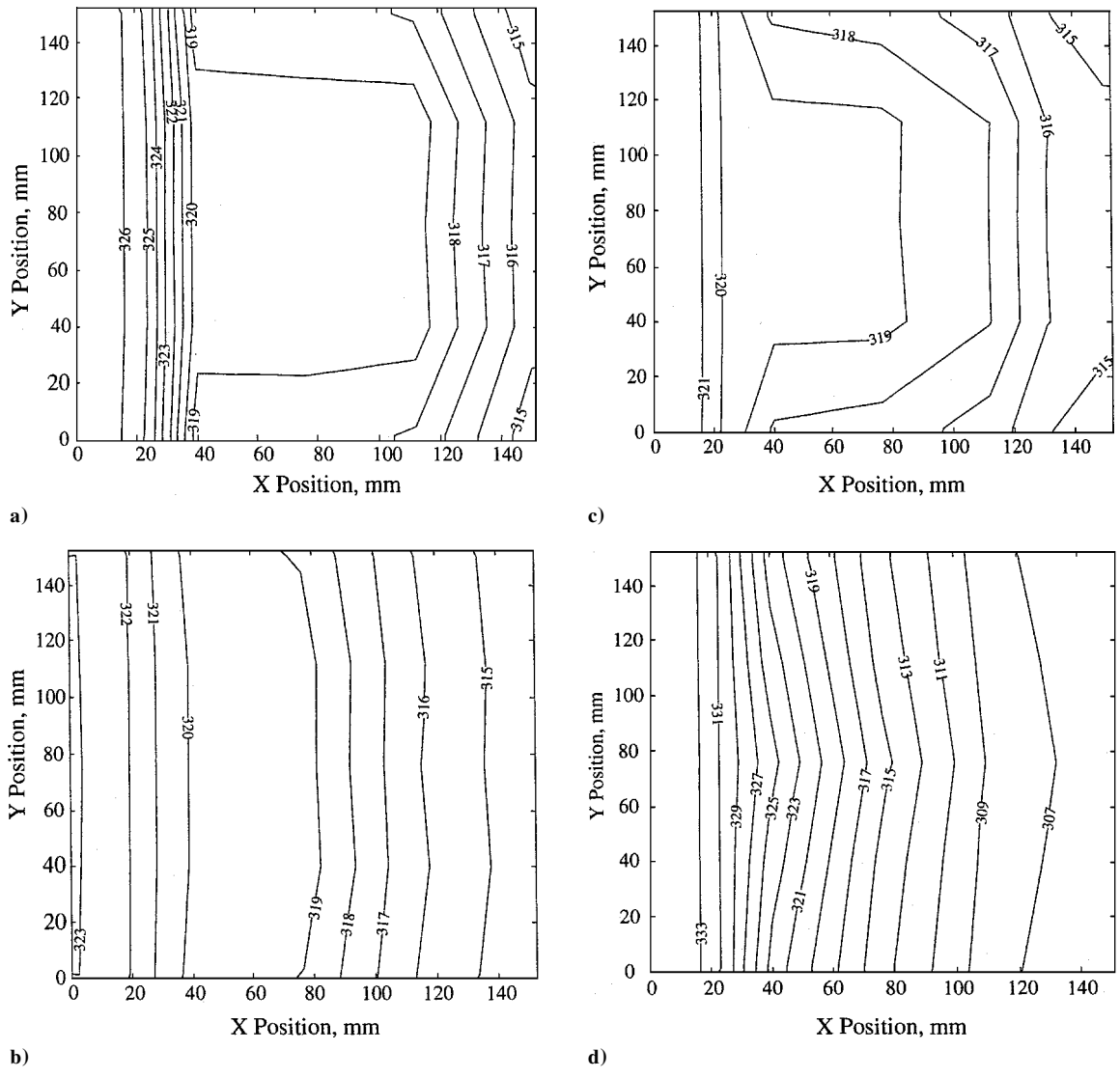

Fig. 3 Two-dimensional temperature distributions on the micro heat pipe radiator with a) $d_w = 0.635$ mm, b) $d_w = 0.813$ mm, c) $d_w = 1.016$ mm, and d) uncharged version at $P_w = 12.0$ W and $T_{sink} = 253$ K.

Results and Discussion

The results from the experimental program are presented first, followed by the analytical and numerical results. A comparison of these results is then presented to determine the accuracy of the modeling techniques presented.

Experimental Results

Temperature Distribution

The temperature distribution on the surfaces of the micro heat pipe radiators were obtained under various conditions. The two-dimensional temperature distributions for TA1, TA2, TA3, and TA4 are illustrated in Figs. 3a–3d, respectively, at the given sink temperature ($T_{sink} = 253$ K) and power input ($P_w = 12.0$ W). It was clear from the results that the temperatures on the evaporator were slightly higher, with a nearly uniform temperature in the center area and a small temperature decrease at the end of the condenser. In addition, the isotherms are evenly distributed in the center region and a little lower at the edges. The highest temperature measured occurred at the end of the evaporator. However, for TA4 (without working fluid) the temperature decreased linearly, as would be expected, from the evaporator to the end of the condenser. The temperature gradient was much higher than for the case of the fully charged radiators. It is apparent that the charged micro heat pipe radiators had a more uniform temperature distribution than the versions without any working fluid before dryout. Furthermore, the micro heat pipe radiator with a larger wire diameter exhibited a more uniform temperature distribution than those with smaller wire diameters. The temperatures on the condenser section were evenly distributed and a little lower at the edge and the end of the condenser.

The maximum temperature, minimum temperature, and mean temperature for TA1 were 326.9, 314.7, and 320.1 K; for TA2 were 323.1, 314.8, and 318.2 K; and for TA3 were 321.7, 314.7, and 318.6 K, respectively. The maximum temperature, minimum temperature, and mean temperature for the version without working fluid (TA4) were 334.8, 305.3, and 319.3 K, respectively.

As observed in the two-dimensional temperature distributions, the micro heat pipe radiators investigated here exhibited an approximately one-dimensional temperature distribution along the wire direction, although the temperatures on the test articles were not absolutely identical. It is more meaningful to use the average transverse temperatures of the heat pipe radiator to compare the overall heat transfer performance. The average temperature distributions along the micro heat pipe radiators investigated earlier are presented in Fig. 4 at $T_{sink} = 253$ K and $P_w = 12.0$ W. The temperature differences from the evaporator to the condenser decreased with increasing wire diameter.

Comparing the three charged micro heat pipe radiators with the version without any working fluid demonstrates that TA3 reaches a much more uniform temperature distribution than the others and

that the micro heat pipe radiators could significantly reduce the temperature difference along the radiators, thereby increasing the radiation efficiency. The maximum temperature differences were 12.2, 9.3, 7.0, and 28.5 K, respectively, for TA1, TA2, TA3, and TA4 in the studied case. Note that, although the radiation power cannot be evaluated exactly by the mean temperature, the measured average temperatures were close to average value at the same conditions. This is consistent with the understanding that the radiation heat transfer depends only on sink temperature and the environmental conditions for a given radiator surface.

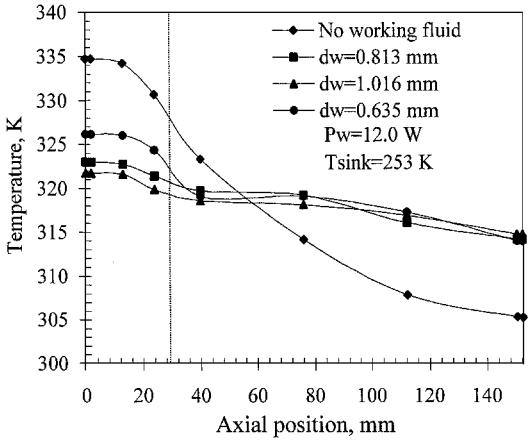

Fig. 4 Comparison of the average temperature distributions on micro heat pipe radiators at T_{sink} = 253 K and P_w = 12.0 W.

Radiation Efficiency

The concept of radiation efficiency is very useful for the design of radiator fins with micro heat pipes used in a space environment. The heat output and heat source temperatures are typically known, making it possible to determine the required heat transfer area. To determine the heat transfer rate of the micro heat pipe array for a given maximum source temperature, the radiation heat transfer at different evaporating temperatures was investigated.

From the definition given by Eq. (4), and employing the experimental data obtained here, the radiation efficiencies for the four test radiators are presented in Fig. 5. As expected, the radiation efficiency of the micro heat pipe radiator without any working fluid is much lower than any of the other micro heat pipe radiators, especially at higher source temperatures. The radiation efficiency decreases with the increasing source temperature regardless of the sink temperature for the uncharged radiator (TA4). However, this is not the case for the micro heat pipe radiators. When the source temperature increases, the radiation efficiency increases before dryout occurs. The maximum radiation efficiency of the micro heat pipe radiator reached a level of 0.95 in the test environment.

Maximum Heat Transport Capacity

The maximum heat transport capacity is the operating limitation of a micro heat pipe radiator that is reached when the capillary force is not large enough to pump sufficient working fluid back to the evaporator. The maximum heat transport capacity depends on the length of the evaporator and condenser sections, the sink temperature, the space between the wires, and the wire diameter. Determination of the maximum heat transport capacity can be accomplished by observing the temperature variation on the evaporator surface.

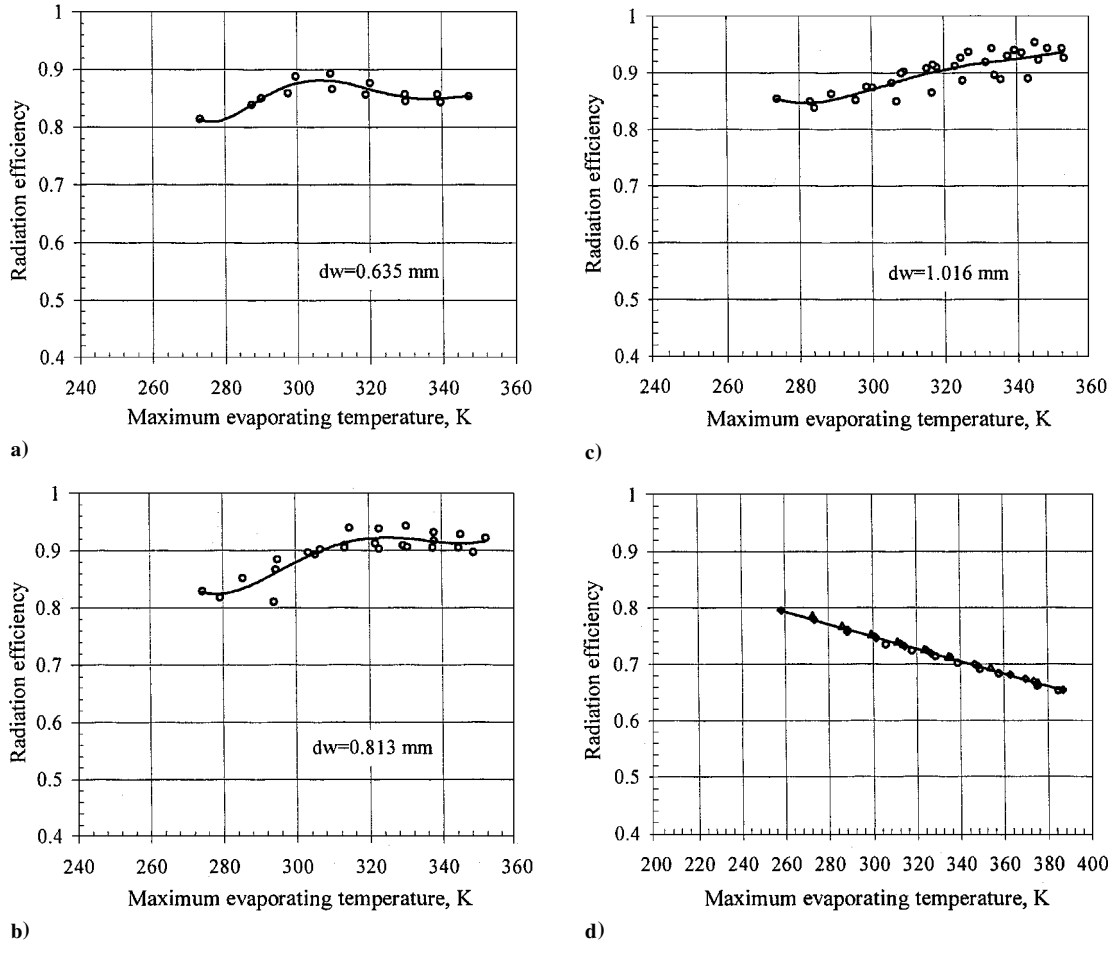

Fig. 5 Radiation efficiencies of the micro heat pipe radiator with a) d_w = 0.635 mm, b) d_w = 0.813 mm, c) d_w = 1.016 mm, and d) uncharged version.

Table 3 Configurations for the studied micro heat pipe radiators

Prototype	Case 1	Case 2	Case 3	Case 4	Case 5	Case 6
Material	Aluminum	Aluminum	Aluminum	Aluminum	Aluminum	Aluminum
Working fluid	Acetone	Acetone	Acetone	Acetone	Acetone	Acetone
Dimension, mm	152.4 × 152.4	152.4 × 152.4	152.4 × 152.4	152.4 × 152.4	152.4 × 152.4	152.4 × 152.4
Thickness of sheet, mm	0.41	0.41	0.41	0.41	0.41	0.41
Diameter of wire, mm	0.330	0.406	0.635	0.813	1.016	1.270
Number of wires	108	96	77	84	73	59
W, mm	1.40	1.60	2.00	1.80	2.10	2.6
Evaporator size, mm	25.4	25.4	25.4	25.4	25.4	25.4
Condenser size, mm	127.0	127.0	127.0	127.0	127.0	127.0

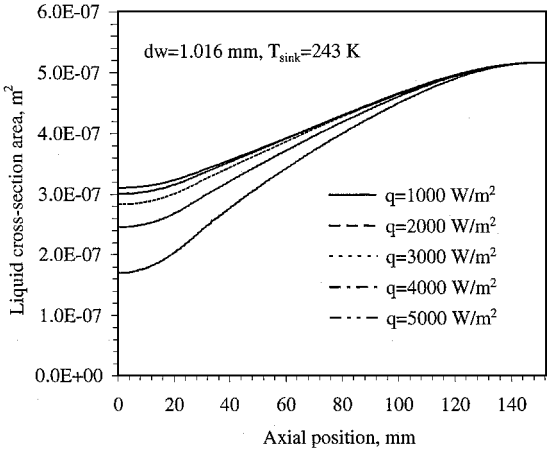

Fig. 6 Liquid distributions in a single channel of the micro heat pipe with d_w = 1.016 mm.

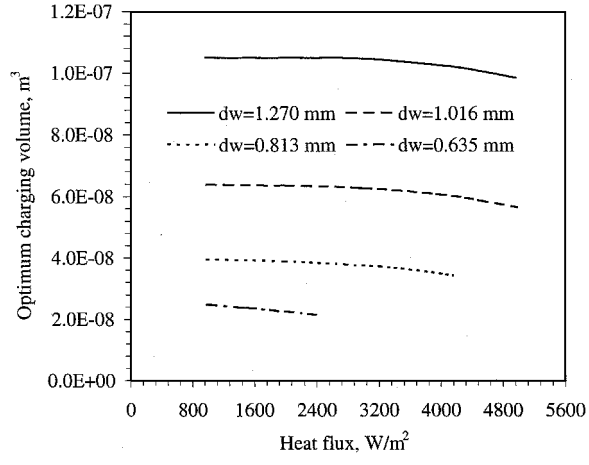

Fig. 7 Optimum charging volume for a single channel in the micro heat pipe radiators.

The temperature at the end of the evaporator increases rapidly when dryout occurs.

The maximum heat transport capacity, as determined in this fashion, was found to increase with increasing wire diameter. In the operating temperature range of acetone, that is, 0–90°C, the observed maximum heat transport capacity for the micro heat pipe radiator with a wire diameter of 0.635 mm was approximately 15.2 W and decreased with decreasing sink temperature. No obvious dryout was observed for the micro heat pipe radiators with wire diameters of 0.813 and 1.016 mm, presumably due to input power limitations.

Modeling Results

By the use of the analytical model, the maximum heat transport capacity of the micro heat pipe radiators was predicted, and the mass distribution and optimum charging volume were estimated. In addition, the optimum design parameters have been obtained in a radiation environment. The configurations of the micro heat pipe radiators studied here are presented in Table 3.

Mass Distributions and Optimum Charging Volume

The distribution of working fluid in the microchannels depends on the geometry of the channel, the heat transport, and the properties of the working fluid. The liquid meniscus radius varies continuously from the condenser to the evaporator due to the frictional pressure drop. The cross-sectional area of the liquid strongly depends on the liquid meniscus radius and the evaporator heat flux. The liquid mass distribution in the microchannel of the micro heat pipe with a wire diameter of 1.016 mm is presented in Fig. 6 as an example. The liquid distribution decreases from the condenser to the evaporator due to the receding of the liquid meniscus and decreases with increasing power input due to increases in the pressure drop.

Note that the amount of working fluid required for proper operation of the micro heat pipe varies due to this change. The ideal operating state of a heat pipe is to have no extra working fluid in the condenser section to block the effective condenser length. The optimum charging quantity can be determined based on this ideal state, and the calculated optimum charging volume of the micro heat pipes are presented in Fig. 7. Because the meniscus radius changes evenly in the condenser section and the length was much longer than the evaporator section, the optimum charging volume changed evenly with increases in the heat flux. The optimum charging ratio, which is defined as the ratio of optimum charge volume and total volume of the channel, varies from 31.8 to 33.9% for micro heat pipes with wire diameters of 1.27 mm, from 28.0 to 31.7% for 1.016 mm, and from 23.7 to 27.5% for 0.813 mm. Note that the penalty for a slight overcharge is a reduction in operational efficiency, whereas the penalty for undercharge is complete failure.

Maximum Heat Transport Capacity

The maximum heat transport capacity of the micro heat pipe radiator is affected by the sink temperature (through the evaporating temperature), the wire diameter, the space between wires, and the length of the micro heat pipe. Investigation of these effects can result in the optimum design of micro heat pipe radiators, thereby reducing the total weight of the radiators.

As previous investigations indicated,[2,6,7,11,12] the maximum heat transport capacity varies with the operating temperature. The operating temperature in a convection environment is typically defined as the average temperature in the adiabatic section; however, there is no adiabatic section when the micro heat pipe is used as a radiator in a space environment. Hence, in this case, the evaporating temperature is used as the operating temperature to estimate the maximum heat transport capacity in a radiation environment.

The predicted maximum heat transport capacity of the micro heat pipes is presented in Fig. 8. Note that the modeling maximum heat transport capacity is just for one channel (single heat pipe). The capacity of the heat pipe radiator should be multiplied by the number of channels in the radiator. The operating temperature of the micro heat pipe in a radiation environment depends primarily on the sink temperature. However, even when the sink temperature was assumed to be very low, the maximum heat transport capacity was not reached

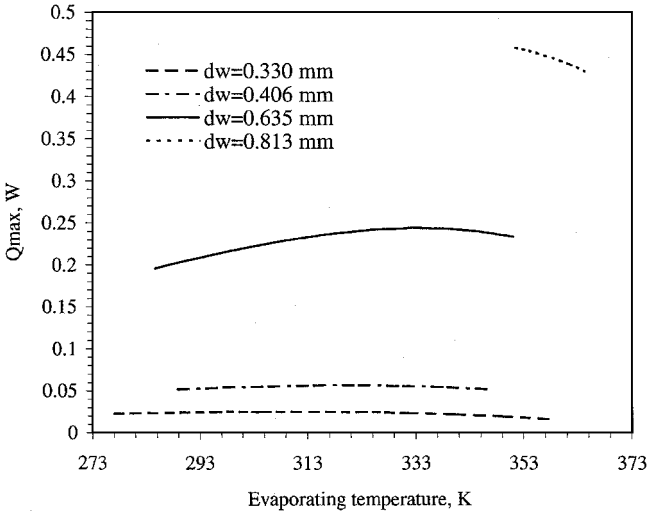

Fig. 8 Maximum heat transport capacities of a single micro heat pipe in the radiators.

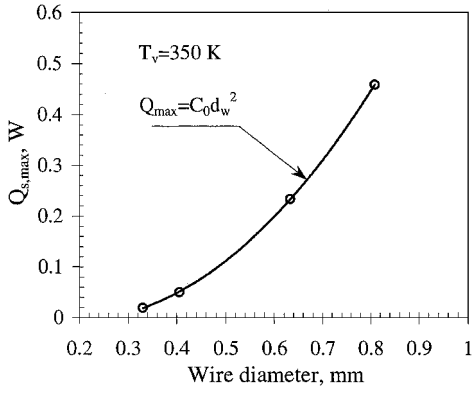

Fig. 9 Effect of wire diameter on the maximum heat transport capacity.

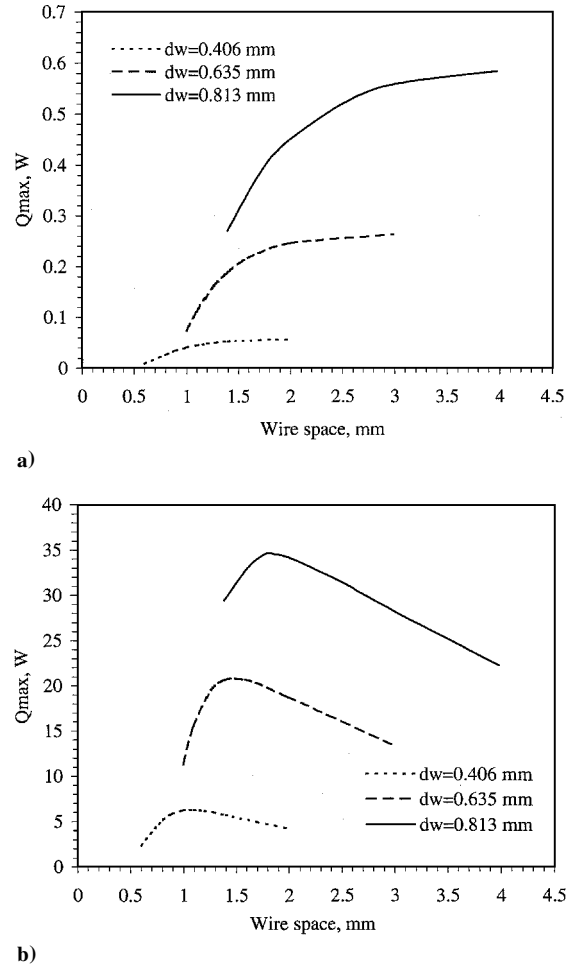

Fig. 10 Effect of the wire space on the maximum heat transport capacity of a) single heat pipes and b) micro heat pipe radiators.

for micro heat pipe radiators with larger wire diameters, such as 1.016 and 1.270 mm (length of 152.4 mm).

The available maximum heat transport capacity for a micro heat pipe with a diameter of 0.813 mm is 0.458 W at 78.9°C and decreases to 0.428 W at 92.4°C. This implies that when the micro heat pipe operates within the temperature range 0–92°C, the radiation heat transport capacity is less than 0.43 W at any sink temperature. The maximum heat transport capacities were obtained for micro heat pipes with wire diameters of 0.635, 0.406, and 0.330 mm. As shown in Fig. 8, the maximum heat transport capacity increases with increases in the evaporating temperature to a maximum value and then decreases. The maximum value for the micro heat pipe with 0.635-mm wires was 0.244 W at 64.4°C. The evaporating temperature corresponding to this maximum value increased with the increases in the wire diameter. For the micro heat pipe with a wire diameter of 0.330 mm, the optimum maximum heat transport capacity was 0.0252 W at 31.3°C. The maximum heat transport capacity increased rapidly with increases in the wire diameter. Further inspection shows that the relationship of the wire diameter to the maximum heat transport capacity is proportional to the square of the wire diameter as illustrated in Fig. 9.

Optimum Design Parameters

As mentioned earlier, the sink temperature, space between wires, and the length of the micro heat pipe all have a significant effect on the maximum heat transport capacity of the micro heat pipe radiator. Therefore, to determine the design of the radiators, the heat transport capacity not only needs to be determined by the limitation of the micro heat pipe, but also the radiation limitation. Increasing the space between the wires can reduce the frictional pressure drop, therefore increasing the maximum heat transport capacity of a single heat pipe, as presented in Fig. 10a. However, the number of heat pipes on the array is decreased. Clearly, there exists an optimum wire spacing where the maximum heat transport capacity of the radiator reaches a maximum value. The variation of the maximum heat transport capacity with wire spacing for three micro heat pipe radiators is shown in Fig. 10b, where the optimum design wire spacing is 1.1, 1.5, and 1.8 mm, respectively, for micro heat pipe radiators with wire diameters of 0.406, 0.635, and 0.813 mm.

In addition to the spacing distance, the total length of the micro heat pipe has a significant effect on the maximum heat pipe capacity. Increasing the length of the heat pipe radiator results in a decrease in the maximum heat transport capacity, as shown in Fig. 11. However, as mentioned earlier, the heat transport capacity of the micro heat pipe radiator is also limited by the radiation capacity of the surface. At a given heat source temperature, the maximum possible heat transport of a radiator is determined by

$$Q_{r,\max} = FA_r\varepsilon\sigma_0\left(T_{e,\max}^4 - T_{\sin k}^4\right) \tag{19}$$

where $T_{e,\max}$ is the maximum evaporating (heat source) temperature on the evaporator section. This implies that at the given evaporating temperature, the micro heat pipe radiator will not reach the capillary limitation if the length of the radiator is less than the length at which the maximum heat transport capacity is equal to the maximum possible radiation. As a result, the optimum length of the micro heat pipe radiator can be determined as illustrated in Fig. 11.

Increasing the length of the radiator can result in a reduction in the number of loop transport tubes required, thereby reducing the total weight of the radiator, as shown in Fig. 12.

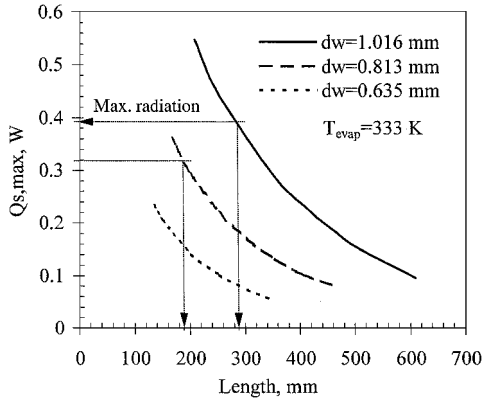

Fig. 11 Effect of length on the maximum heat transport capacity.

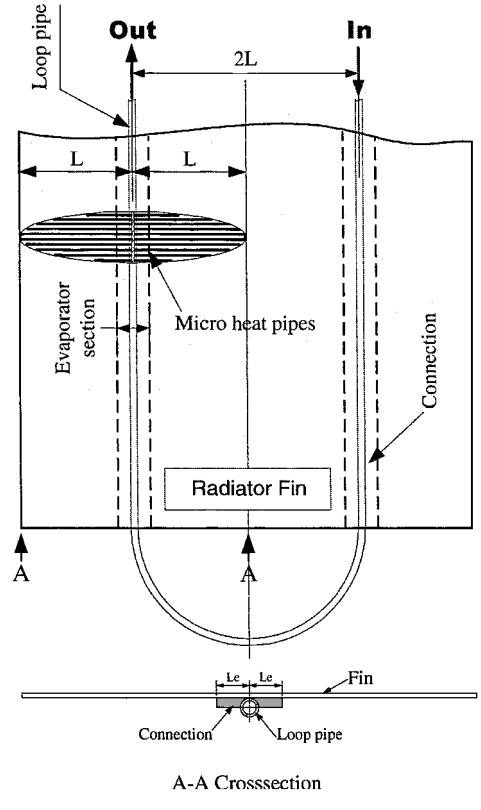

Fig. 12 Schematic of the assembly of a micro heat pipe radiator fin.

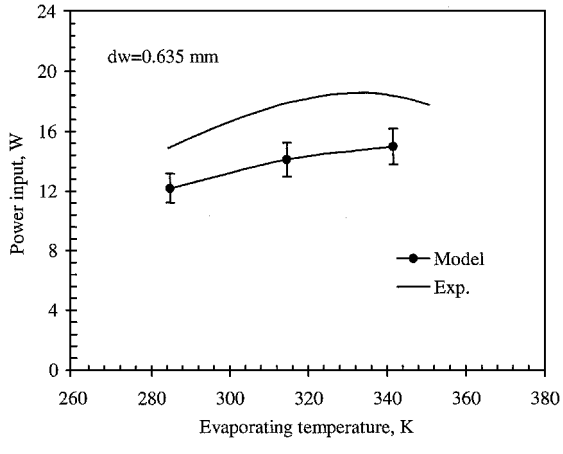

Fig. 13 Comparison of the predicted and experimental results of maximum heat transport capacities of the micro heat pipe radiator with d_w = 0.635 mm.

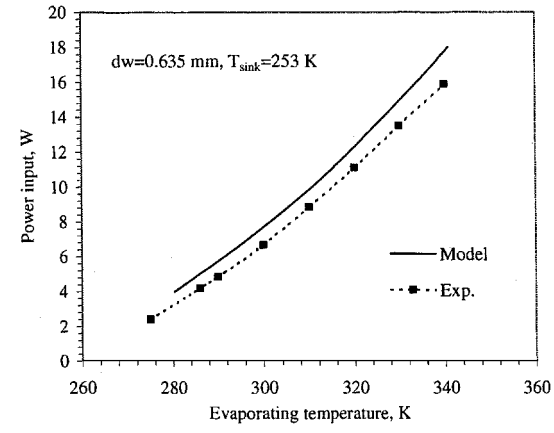

a)

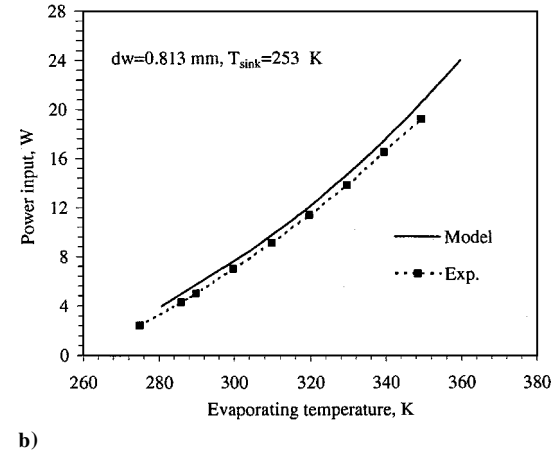

b)

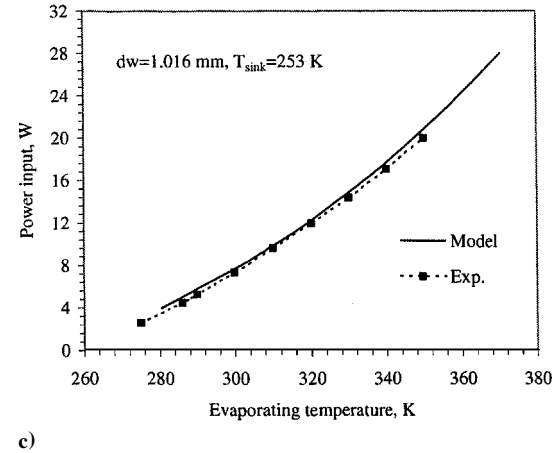

c)

Fig. 14 Comparison of the predicted radiation transfer with experimental results for the micro heat pipe with a) d_w = 0.635 mm, b) d_w = 0.813 mm, and c) d_w = 1.016 mm.

Comparison of Results

To verify the validity of the model, the predicted maximum heat transport capacity of a micro heat pipe with a wire diameter of 0.635 mm was compared with the measured experimental results. As presented in Fig. 13, the predicted maximum heat transport capacity is somewhat larger than the measured experimental results. The maximum deviation was 19.62%. Further tests were conducted to compare the radiation heat transfer of micro heat pipes at various evaporating temperatures. These results are presented in Fig. 14a, 14b, and 14c for wire diameters of 0.635, 0.813, and 1.016 mm. The predicted results were quite close to the experimental results for a wire diameter of 0.813 and 1.016 mm, and the experimental results for the radiator with a wire diameter of 0.635 mm were lower than the predicted results.

Conclusions

A series of wire-bonded micro heat pipe radiators designed for use in lightweight, flexible radiators for long-term spacecraft missions have been developed and investigated, both experimentally and analytically. A detailed experimental investigation was conducted, and the results indicated that the maximum heat transport capacity and radiation efficiency both increased with increasing wire diameter. The maximum heat transport capacity of the radiator utilizing a wire diameter of 0.635 mm was approximately 15.2 W. Radiators utilizing a wire diameter of 0.813 and 1.016 mm never reached the maximum heat transport capacities for the given test conditions due to the length of the radiator. Sink temperatures determined the evaporating temperature of the micro heat pipe radiator and were also shown to affect the maximum heat transport capacity. In the experimental tests, temperature distributions were recorded for several sink temperatures and indicated that, as the sink temperature was reduced, the maximum heat transport capacity and radiation efficiency also decreased. Comparison of the micro heat pipe radiators with and without working fluid indicated that significant improvements in temperature uniformity and radiation efficiencies could be obtained, especially at higher heat fluxes. A maximum radiation efficiency of 0.95 was observed. In general, although some variation was observed, all three micro heat pipe radiators were found to be capable of meeting the thermal requirement of long-term space missions.

In addition to the experimental evaluation, a one-dimensional analytical model was developed to study the heat transfer performance and optimize the design parameters of the micro heat pipe radiator in a radiation environment. Distribution of working fluid, optimum charging quantity, and the maximum heat transport capacity were obtained in a radiation environment. In addition, the effects of operating temperature, wire diameter, spacing between the wire, and length of the radiator were also investigated. The optimum charging volume of the micro heat pipe radiator was shown to be affected by the operating condition and decreased slightly with increasing heat flux. The predicted results indicated that maximum heat transport capacity increased with increases in wire diameter and was proportional to the square of the wire diameter in radiation environments. When the wire diameter is less than 0.330 mm, the maximum heat transfer capacity is less than 0.025 W and will not be capable of meeting the thermal requirements of spacecraft as described earlier. In addition, the maximum heat transport capacity increased with increases in the evaporator temperature to a maximum value and then decreased within the temperature range of acetone. That is, there exists an optimum evaporator temperature at the point where the maximum heat transport capacity reaches a maximum value. This optimum evaporating temperature increases with increases in wire diameter. For micro heat pipe radiators with larger wire diameters, such as 0.813 mm, the maximum heat transport capacity may not be reached in a radiation environment.

The spacing between the wires has a significant effect on the maximum heat transport capacity. Increasing the spacing can increase the maximum heat transport capacity of a single micro heat pipe; however, at some point, this improvement is overshadowed by the decrease in the number of heat pipes in the array, and the maximum heat transport capacity becomes limited. This implies that the maximum heat transport capacity of the micro heat pipe radiator depends not only on the maximum heat transport capacity of a single micro heat pipe, but also on the total number of the micro heat pipes in the array. The optimum spacing distance between two wires for micro heat pipe radiators with wire diameters of 0.813, 0.635, and 0.406 mm were 1.8, 1.5, and 1.1 mm, respectively. The radiative limitation of the radiator surface can be used to optimize the length of micro heat pipe radiator, and, therefore, to reduce the total weight of the radiator assembly.

Overall, the comparison of the predicted results with experimental results shows that the model exhibits good agreement with the experimental results for maximum heat transport capacity.

Acknowledgment

The authors acknowledge the support of National Science Foundation and the Office of Naval Research for the support of this work.

References

[1]Wang, Y., Ma, H. B., and Peterson, G. P., "Investigation of the Temperature Distributions in Radiator Fins with Micro Heat Pipes," *Journal of Thermophysics and Heat Transfer*, Vol. 15, No. 1, 2001, pp. 42–50.

[2]Babin, B. R., Peterson, G. P., and Wu, D., "Steady-State Modeling and Testing of a Micro Heat Pipe," *Journal of Heat Transfer*, Vol. 112, No. 3, 1990, pp. 595–601.

[3]Wu, D., and Peterson, G. P., "Investigation of Transient Characteristics of Micro Heat Pipes," *Journal of Thermophysics and Heat Transfer*, Vol. 2, No. 5, 1991, pp. 129–134.

[4]Peterson, G. P., and Mallik, A. K., "Transient Response Characteristics of Vapor Deposited Micro Heat Pipe Arrays," *Journal of Electronic Packing*, Vol. 117, No. 1, 1995, pp. 82–87.

[5]Peterson, G. P., "An Introduction to Heat Pipes," Luikov Heat and Mass Transfer Inst., Byelorussian Academy of Sciences, Paper A-4, May 1990.

[6]Ma, H. B., and Peterson, G. P., "Experimental Investigation of Thermal Capillary Limit of a Novel Micro Heat Pipe Design," AIAA Paper 97-0979, Jan. 1997.

[7]Longtin, J. P., Badran, B., and Gerner, F. M., "A One-Dimensional Model of Micro Heat Pipe During Steady-State Operation" *Journal of Heat Transfer*, Vol. 116, No. 3, 1994, pp. 709–715.

[8]Wang, Y. X., and Peterson, G. P., "Analysis of Wire-Bonded Micro Heat Pipes" *Journal of Thermophysics and Heat Transfer*, Vol. 16, No. 3, 2002, pp. 346–355.

[9]Peterson, G. P., "Analytical and Experimental Investigation of Micro Heat Pipe," Luikov Heat and Mass Transfer Inst., Byelorussian Academy of Sciences, Paper A-10, May 1990.

[10]Peterson, G. P., and Ma, H. B., "The Theoretical Analysis of the Maximum Heat Transport in Triangular Grooves—A Study of Idealized Micro-Heat Pipes," *Journal of Heat Transfer*, Vol. 118, No. 3, 1996, pp. 731–739.

[11]Fagri, A., *Heat Pipe Science and Technology*, Taylor and Francis, Washington, DC, 1995, pp. 636–655.

[12]Khrustalev, D., and Fagri, A., "Thermal Analysis of Micro Heat Pipe," *Journal of Heat Transfer*, Vol. 116, No. 1, 1994, pp. 189–198.